A Framework of Electricity Market Based on Two-Layer Stochastic Power Management for Microgrids

MEHDI VEISI[1], **FARID ADABI**[1], **ABDOLLAH KAVOUSI-FARD**[2], (Senior Member, IEEE),
AND MAZAHER KARIMI[3], (Senior Member, IEEE)

[1]Department of Electrical Engineering, Sanandaj Branch, Islamic Azad University, Sanandaj 66169-35391, Iran
[2]Department of Electrical and Electronics Engineering, Shiraz University of Technology, Shiraz 71557-13876, Iran
[3]School of Technology and Innovations, University of Vaasa, 65200 Vaasa, Finland

Corresponding authors: Farid Adabi (farid.adabi@iau.ac.ir) and Mazaher Karimi (mazaher.karimi@uwasa.fi)

ABSTRACT This Article Develops a Novel Multi-Microgrids (MMGs) Participation Framework in the Day-Ahead Energy and Ancillary Services, i.e. Services of Reactive Power and Reserve Regulation, Markets Incorporating the Smart Distribution Network (SDN) Objectives Based on Two-Layer Power Management System (PMS). A Bi-Level Optimization Structure Is Introduced Wherein the Upper Level Models Optimal Scheduling of SDN in the Presence of MMGs While Considering the Bilateral Coordination Between Microgrids (MGs) and SDN's Operators, i.e. Second Layer's PMS. This Layer Is Responsible for Minimizing Energy Loss, Expected Energy Not-Supplied, and Voltage Security as the Sum of Weighted Functions. In Addition, the Proposed Problem Is Subject to Linearized AC Optimal Power Flow (LAC-OPF), Reliability and Security Constraints to Make It More Practical. Lower Level Addresses Participation of MGs in the Competitive Market Based on Bilateral Coordination Among Sources, Active Loads and MGs' Operator (First Layer's PMS). The Problem Formulation Then Tries to Minimize the Difference Between MGs' Cost and Revenue in Markets While Satisfying Constraints of LAC-OPF Equations, Reliability, Security, and Flexibility of the MGs. Karush–Kuhn–Tucker Method Is Exploited to Achieve a Single-Level Model. Moreover, a Stochastic Programming Model Is Introduced to Handle the Uncertainties of Load, Renewable Power, Energy Price, the Energy Demand of Mobile Storage, and Availability of Network Equipment. The Simulation Results Confirm the Capabilities of the Suggested Stochastic Two-Layer Scheme in Simultaneous Evaluation of the Optimal Status of Different Technical and Economic Indices of the SDN and MGs.

INDEX TERMS Two-layer power management system, energy and ancillary services markets, multi-criteria objectives, multi-microgrids, multi-objective bi-level optimization.

NOMENCLATURE
Abbreviation

AC-OPF	AC Optimal Power Flow.
ADN	Active Distribution Network.
ARO	Adaptive Robust Optimization.
CHP	Combined Heat and Power.
DA	Day-Ahead.
DER	Distributed Energy Resource.
DG	Distributed Generation.
DHN	District Heating Network.
DRP	Demand Response Program.
DSO	Distribution System Operator.
EEL	Expected Energy Loss.
EENS	Expected Energy Not-Supplied.
EMS	Energy Management System.
ESS	Energy Storage System.
EV	Electric Vehicle.
FDT	Fuzzy Decision-Making Technique.
FOR	Force Outage Rate.
FS	Flexible Source.
GWO	Gray Wolf Optimization.
IBF	Interactive Benefit Prioritization.
KKT	Karush–Kuhn–Tucker.
LAC-OPF	Linearized AC Optimal Power Flow.
MG	Microgrid.

The associate editor coordinating the review of this manuscript and approving it for publication was Salvatore Favuzza.

MGO	Microgrid Operator.
MMG	Multi-Microgrid.
MOV	Maximum Overvoltage.
MVD	Maximum Voltage Drop.
NRDG	Non-Renewable Distribution Generation.
PDF	Probability Distribution Function.
PDN	Power Distribution Network.
PMS	Power Management System.
RDG	Renewable Distribution Generation.
RWM	Roulette Wheel Mechanism.
SBM	Simultaneous Backward Method.
SDN	Smart Distribution Network.
TLBO	Teaching–learning-based Optimization.
VSI	Voltage Security Index.
WSI	Worst Security Index.

Indices and sets

b, i, t, ω	Indices for Buses, MGs, Operation Hours, and Scenario Samples.
j	an Auxiliary Index Representing the Bus.
p, m	The Index Related to the Piecewise Linear in the Conventional Piecewise Linearization Method, and the Index for Sides of a Regular Polygon.
$Pb, Pb\text{-}1$	The Weak Bus in Terms of Voltage Magnitude, and the Bus Upstream of pb.
O_B, O_{MG}, O_{OH}, O_S	Sets of Buses, MGs, Operation Hours, and Scenario Samples.
O_B^{MG}	Set of MG Buses.
O_P, O_M	The Set Related to the Piecewise Linear in the Conventional Piecewise Linearization Method, and the Set of Sides of a Regular Polygon.

Variables

$EEL, EENS, VSI$	Expected Energy Loss (MWh), Expected Energy Not-Supplied (MWh), and Voltage Security Index (Dimensionless).
F_1	The Sum of Energy Loss, Expected Energy Not-Supplied, and Voltage Security Based on the Sum of Weighted Functions Method (Dimensionless).
F_2	The Difference Between the Expected Operation Cost of Non-Renewable Sources and Expected Revenue of MGs From Energy, Reactive Power, and Reserve Market ($).

L_{NS}	Active Power Not-Supplied in per-Unit (p.u.).
P_{CH}, P_{DIS}	Active Charging and Discharging Power of the Storage System (p.u.).
P_{DS}, P_{MG}, P_L	Active Power of the SDN's Substation, MG's Substation, and the Distribution Line.
P_{NR}, P_{DR}	Active Power of Non-Renewable Source and Active Power of Responsive Loads in the Demand Response Program (p.u.).
$Q_{DS}, Q_{MG}, Q_L,$ Q_{NR}, Q_R, Q_E	Reactive Power of the SDN's Substation, MG's Substation, Distribution Line, Non-Renewable Source, Renewable Source, and Storage's Charger (p.u.).
R_{MG}	Reserve Power of the MG Seen From the MG's Substation (p.u.).
$V, \Delta V$	Magnitude and Deviation of Voltage (p.u.).
φ	Voltage Angle (Rad)
WSI	the Worst Security Index (Dimensionless).

Constants

A_L	The Incidence Matrix of Buses and Distribution Lines (if There Is a Line Between Buses b and j, $A_{Lb,j} = 1$, Otherwise, It Is Equal to zero).
A_{MG}	The Incidence Matrix of MGs and Buses in the SDN (if MG i Connects to Bus b, $A_{MGb,i} = 1$, Otherwise It Is Equal to zero).
B_L, G_L	Susceptance and Conductance of the Distribution Line (p.u.).
$\underline{E}, \bar{E}, IE$	Minimum Energy Storable in the Storage, Size (Maximum Storable Energy) of the Storage, and Initial Energy of the Storage (MWh).
$EENS^{max}$	Maximum Energy Not-Supplied (MWh).
K_Q, K_R	The Ratio Between the Reactive Power Price and the Energy Price, the Ratio Between the Reserve Price and the Energy Price (Dimensionless).
L_P, L_Q	Active and Reactive Load (p.u.).
n_p	The Number of Linear Pieces in the Conventional Piecewise Linearization Technique.
P_R	Active Power of the Renewable Source (p.u.).
R, X	Resistance and Reactance of the Distribution Line (p.u.).

s, s'	The Slope of the Line Used for Linearizing a Second and Fourth Power Variable Based on the Conventional Piecewise Linearization Technique.
$\bar{S}_{DS}, \bar{S}_{MG}, \bar{S}_L,$ $\bar{S}_{NR}, \bar{S}_R, \bar{S}_E$	Size (Maximum Apparent Power) of the SDN's Substation, MG's Substation, Distribution Line, Non-Renewable Source, Renewable Source, and Storage's Charger (p.u.).
V_{min}, V_{max}	Lower and Upper Limits of Voltage Magnitude (p.u.).
WSI^{min}	the Minimum Value of WSI.
α_{CR}, α_{DR}	Charging and Discharging Rates of the Storage (p.u.).
β	Fuel Price of the Non-Renewable Source ($/MWh).
$\beta_{DS}, \beta_{MG}, \beta_L$	Availability of the SDN's Substation, MG's Substation, and Distribution Line.
γ	Energy Price ($/MWh).
η_{CH}, η_{DIS}	Charging and Discharging Efficiency of the Storage Device.
π	The Probability of Occurrence of a Scenario.
$\vartheta_{EEL}, \vartheta_{EENS}, \vartheta_{VSI}$	Weighted Coefficients.
ξ	the Participation Rate of Consumers in the DRP.
ΔF	Flexibility Tolerance.
$\Delta\theta, n_m$	Angle Deviation (rad), and the Number of Sides of the Regular Polygon, $\Delta\theta = 360/n_m$.

I. INTRODUCTION

To Achieve Clean Energy Supply Conditions in the Power System and Prevent Early Exhaustion of Fossil Fuels, the Utilization of Environmentally-Friendly Technologies Such as Electric Vehicles (EVs) and Renewable Distribution Generations (RDGs) Placed at Consumption Sites Is a Promising Solution [1]. Thanks to Their Low Emission Level, Non-RDGs (NRDGs), Such as Fuel Cells and Microturbine, Are Widely Used at Consumption Points to Supply Energy as Concentrated Power Plants [1]. In This Regard, Energy Storage Systems (ESSs) and Demand Response Programs (DRPs) Are Highly Potential Choices [1]. Nevertheless, Achieving Desirable Environmental Conditions Besides Improving Technical and Economic Situations of Energy Networks Requires Appropriate Energy Management of These Elements Within the Network. Hence, the First Step Is to Integrate These Elements in Different Coordinating Forms Like Micro-Grids (MGs) [2]. Following This, a Distribution Network Is Expected to Consist of Several MGs. In This Scheme, an MG Is Composed of a Specific Number of Sources,

Storages, and Consumers, Each With Its Local Controller. Moreover, the MG Itself Has a Central Controller Known as the MG Operator (MGO). By Executing Smart and Communication Infrastructure in the MG, It Is Expected That Bilateral Coordination Is Met Among Sources, Storages, and Consumers With the MGO [3]. In This Case, by Adopting an Energy Management System (EMS) or Power Management System (PMS) in the Second Step, an MG With Various Capabilities in Economic and Technical Terms Such as Operation, Reliability, and Security Can Be Obtained [4]. Additionally, Several MGs or Multi-MGs (MMGs) Have Bilateral Coordination With the Distribution System Operator (DSO) in This Scheme; Thus, It Is Predicted That a Suitable Situation From DSO's Viewpoint Is Obtained for the Distribution Network in These Conditions [5].

A Great Deal of Research Has Been Conducted on the Management of the Operation of Distribution Networks or MGs. To Exploit a Mixture of Active and Reactive Power Control Capabilities of EVs, a Model Is Introduced in [6] to Manage These Powers Simultaneously in an Smart Distribution Network (SDN). The Model Forms an Optimization Formulation, the Objective Function of Which Attempts to Minimize the Energy Cost and Improve Voltage Profile. The Problem Is Subject to Operation Constraints of the Network and Charging and Discharging Constraints of EVs Batteries and Chargers. Adopting the Adaptive Robust Optimization (ARO), the Authors in [7] Put Forward a Model to Optimally Schedule an Active Distribution Network (ADN) Composed of RDGs and Flexible Sources (FSs). An Optimization Model With Two Objective Functions Is Used in the Deterministic Programming to Minimize the Difference Between the Operating Costs of the Network and NRDGs and the Revenue of the RDG, NRDG, and FS Gained by Selling Active and Reactive Power (the First Objective function). The Voltage Deviation Is Minimized by the Second Objective Function. The Problem Takes Into Account the AC Optimal Power Flow Constraints for the ADN With RDGs and FSs. Uncertainties of the Load, Market Price, EVs, and RDG Specifications Are Also Considered in the Problem; Hence, the ARO Was Adopted to Model/Find Uncertainty Parameters/Robust Capabilities of Renewable and Flexible Sources Aiming to Enhance the Status of the Network's Operation Indices. An Energy Management System Is Used for the Optimal Multi-Objective Operation of MGs With Distributed Generations (DGs) and a Thermal Block [8]. A Combined Heat and Power (CHP) System, a Boiler, and a Thermal Storage System Supply the Load of the Thermal Block. The Proposed Solution Minimizes Three Operation Objectives of an MG: Cost, Energy Loss, and Voltage Deviation Functions. The Problem Is Constrained by AC Power Flow Equations, System Operation Limits, and Limitations on DGs and the Thermal Block. Then, the teaching–learning-based Optimization (TLBO) and Firefly Algorithm Are Incorporated to Solve the Problem and Achieve a Reliable Optimal Solution. Interconnected Power Distribution Network (PDN) and District Heating Network (DHN) Infrastructures Through

CHP Units and Heat Pumps Are Discussed in [9]. Accessing Nodal Electricity Prices in the Market Framework, the DHN's Operator Solves an Optimal Thermal Flow Problem and Explores the Best Strategy for Generating Heat. The Performance Factors of Heat Pumps Concerning Variable Load Levels Are Taken Into Account and Modeled by a Disciplined Convex Optimization Format. A Two-Step Hydraulic-Thermal Decomposition Method Is Used to Find the Solution for the Optimal Thermal Flow Problem via a Quadratic Cone Program. Meanwhile, the PDN's Operator Clears the Distribution Power Market Using an Optimal Power Flow Problem Considering the DHN's Demand. Electrical Energy Prices Are Represented Using Dual Variables in the Optimal Solution. The Problem Results in a Nash-Type Game Between the Two Systems. Then, a Best-Response Decentralized Algorithm Is Adopted to Find the Optimal Operation Scheduling of the Infrastructure, Which Interprets a Market Balance Because None of the Systems Is Inclined to Change Their Strategies. Taking Into Account the Electrical Energy Price Response of Distributed Energy Resource (DER), a Coordinated Operation Strategy for ADN Is Presented Based on a Bi-Level Agent Framework [10]. The DER Agent Responds According to the Technical Operability and Economic Consideration, While the ADN Agent Will Finally Coordinate Each Participant by Using the Interactive Benefit Prioritization (IBP) Principle.

The Authors in [11] Present an Optimal Scheduling Model for an MG That Is Involved in Electrical Energy Distribution Market, in Which the Distribution Market Operator Is Also Participates. To Minimize the Operation Cost of off-Grid MGs, Ref. [12] Models the Spinning Reserve Uncertainty and Employs a Novel Optimal Scheduling Model. In This Method, the Confidence Levels Related to Probability Constraints of Spinning Reserve Are Suitably Set; Thus, the MG Finds a Compromised Solution Between Reliability and Economic Situation. Cooperative Operation of Several MGs That Work Interconnected Is Optimally Scheduled in [13]. The Proposed Structure Minimizes the Expected Profit of Individual MGs and Reduces the Power Loss of the Distribution System. Reconfiguration of MGs Is Realized in [14] by Using a Strategy While Taking Into Account the Capability Constraints of Islanding. To This End, the Capability of Islanding Is Modeled by a Probability of Islanding Operation Index to Present the Probability of Sufficient Spinning Reserve of the MG in Supplying the Required Demand. An Energy Management System (EMS) Is Used Has Also Been Adopted [15] to Find Highly Reliable MGs With Pollution-Less Energy and Optimal Operation. Another Interesting Method Called Stochastic Multi-Layer Energy Management Was Incorporated in [16] to Interconnected MGs Operating Based on Smart Distribution Networks. Energy Management Was Realized by Individual MGs Aiming to Specify the Suitable Scheduling of MGs' Units. The Operator of the Smart Network Uses the Received Data to Prepare a Priority List for Units That Can Inject Power Into the Smart Network. Then, Energy Is Globally Managed.

In an Attempt to Enhance Reliability of MGs, Make Their Operation Optimum, and Use Clean Energy, the Multi-Objective Operation Is Introduced for MMGs [17]. Such an Operation Helps Minimize the Expected Operating Cost of MGs and Non-Renewable Energy Sources (NRESs), the Expected Energy Not-Supplied (EENS) as the Reliability Index, Expected Environmental Emission Level, and Voltage Deviations Function in Different Objective Functions. The Problem Is Limited by AC Optimal Power Flow (AC-OPF) Equations, Constrictions of Reliability, and Mathematical Models of Power Sources and Active Loads. The Authors in [18] Propose a Similar Study Although It Uses an Unbalanced Model for MGs. A Novel Energy Management Method With Two Stages Is Introduced for Interconnected MGs With the Penetration of High Renewables. The Aim Is to Deal With the Stochastic Changes of Renewable Energy Output Occurring During the Day, Changes in the Electrical Demand, and Electricity Price. The First Stage (With Hourly Step Intervals) Adopts a Hierarchical Hybrid Control Method for Interconnected MGs so That the Operating Cost of the System Is Minimized. To Evaluate the Risk of Changes in the Operating Cost Caused by Uncertainties, the mean–variance Markowitz Theory Is Utilized. The Second Stage (with 5-min Step intervals) Adjusts the Elements of MGs in an Optimal Way so That the Imbalance Cost Between Day-Ahead and Real-Time Markets Is Minimized. Ref. [20] Proposes a New Operation Method for Grid-Connected MGs Highly Influenced by Renewables and Electric Vehicles for Day-Ahead and Real-Time Markets, in Which MGs Are Managed via a Multi-Layer EMS. In This Approach, MGs Are Either Single MGs or Interconnected MGs. Single MGs Are Managed Through the First Layer of the EMS, While the Interconnected MGs Are Managed Using the Second Layer and This Is Realized in Hourly Based in the day-ahead market.

Table 1 Tabulates the Studied Carried Out in This Realm.

In the Field of Energy Management of Distribution Networks and MGs, Different Models in Proportion to the Background Research Are Provided in the Literature Review Section and Table 1. However, the Noticeable Research Gaps Concerning Energy Management of Distribution Network and MGs Include the Following Items:

- Most Studies Employ Integrated or Single-Layer Management for Distribution Networks or MGs. Such Management Strategy Considers Only the Direct Coordination Between Sources and Active Loads and the DSO. Nonetheless, Implementing Such Coordination in the Distribution Network With MMGs, i.e. Realization of Coordination Between Sources and Active Loads and the DSO, Leads to a Huge Volume of Data for the DSO, Thus Complicating the Decision-Making Procedure and System Processing by the DSO. Therefore, the Optimal and Desirable Conditions Are Those With a Two-Layer PMS to Manage Distribution Network Power in the Presence of MMGs. In This Type of Scheme, the Coordination Between Sources and Active Loads and the MGO Is Considered in One Layer of the

TABLE 1. Taxonomy of recent research works.

Ref.	Indices					Market model	PMS strategy
	Economic	Operation	Security	Reliability	Flexibility		
[6]	Yes	Yes	No	No	No	Energy	One-layer
[7]	Yes	Yes	No	No	No	Energy and reactive	One-layer
[8]	Yes	Yes	No	No	No	-	One-layer
[9]	Yes	Yes	No	No	No	Energy	One-layer
[10]	No	Yes	No	No	Yes	-	Two-layer
[11]	Yes	Yes	No	No	No	Energy	One-layer
[12]	Yes	Yes	No	Yes	No	-	One-layer
[13]	Yes	Yes	No	No	No	Energy	One-layer
[14]	Yes	Yes	No	Yes	No	-	One-layer
[15]	Yes	Yes	No	Yes	No	-	One-layer
[16]	Yes	Yes	No	No	No	-	Two-layer
[17-18]	Yes	Yes	No	Yes	No	-	Two-layer
[19-20]	Yes	Yes	No	No	No	Energy	Two-layer
Proposed strategy	**Yes**	**Yes**	**Yes**	**Yes**	**Yes**	**Energy, reactive and reserve**	**Two-layer**

PMS While the Coordination of MGOs and the DSO Is Assumed in the Other Layer. Thus, It Is Anticipated That the Decision-Making Speed and Operators' Processing Actions Are High Thanks to Dividing and Sharing the Whole Data of System Players Among Several Operators. This Has Been Discussed in Few Studies Such as in [10], [16]–[20]. But, in [17], [18] / [10], [19], [20], the Multi-Bus Mode of Distribution Network / MGs Is Not Considered.

- As It Was Observed in the Literature Review Section, Implementing Energy Management in MGs Helps Improve the Technical Status of the Distribution Network. So, MGs Can Participate in Different Energy Markets and Enhance Their Financial Benefit. Yet, Most Research Pieces Generally Use the Energy Market Model for MGs. MGs Using Base Generator Sources Such as Microturbines and Based Inverter Elements Such as Renewables, ESSs, and EVs Can Control Active and Reactive Power Simultaneously [21]. Hence, They Can Participate in Active Ancillary Services Markets Such as Reserve Regulation and Reactive Ancillary Services, in Addition to Participating in the Energy Market.

- In Most Studies [6]–[9], [11], [13], [16], the Optimal Status of One or Two Indices Such as Economic and Operation Indices Are Generally Taken Into Account. However, a Network Is Subject to Various Indices Including Reliability, Security, Flexibility, Operation, etc. Achieving a Suitable Situation of a Specific Index Does Not Guarantee to Enhance the Status of Another Index. For Instance, High Amounts of Energy Need to Be Injected by Sources, and Active Loads Placed at Consumption Points to Improve Reliability. But From an Operation Aspect, This May Result in Overvoltage. So, It Is Expected to Consider Simultaneous Modeling of Different Indices in the Problem of Management of Network Power.

To Fill the Aforementioned Gaps, the Present Study Suggests the Participation of SDN-Connected MMGs in the Energy and Ancillary Services, i.e. Services of Reactive Power and Reserve Regulation, Markets Using a Two-Layer PMS, as Shown in Fig. 1. In the Proposed Scheme, the PMS's First Layer Refers to the Bilateral Coordination Between Sources, Storages, and Responsive Loads and the MGO, While the Bilateral Coordination of MGOs and the DSO Is Considered in the Second Layer of the PMS. Then, First (Second) Layer of PMS Based on Fig. 1 Refer to Active and Reactive Power Management Is MG (SDN). It Is a Bi-Level Problem, in Which the Upper Level Deals With the Optimal Scheduling Modeling of the SDN in the Presence of MMGs Based on the Second Layer's PMS, That Is the Coordination Between MGOs and the DSO. In the Formulation of the Lower Level, the Participation of MMGs in the Day-Ahead (DA) Energy, Reactive Power, and Reserve Markets Is Modeled Based on the First Layer's PMS, i.e. According to the Coordination of Sources and Active Loads and the MGO. The Objective Function in the Upper Level Aims to Minimize the Total Loss of Energy, Reliability, and Network Security, Formulated in the Form of Pareto Optimization Based on the Sum of Weighted Functions Technique. Moreover, It Is Subject to the AC Optimal Power Flow (AC-OPF) Equation and Constraints of Reliability and Voltage Security in the Presence of MGs' Data. In the Lower Level, the Objective Function Attempts to Minimize the Difference Between the Expected Cost of MGs and Their Expected Revenue in the Mentioned Markets, Constrained to AC-OPF Equations, Equations Ruling the Renewable and Non-Renewable Sources, and Active Loads Such as ESSs, EVs Parking Lot, DRP, Reserve Model of the MG, and Constraints of Reliability, Security, and Flexibility of MGs. To Find an Integrated and Single-Level Model, the Karush–Kuhn–Tucker (KKT) Technique Is Adopted. The Lower Level Problem Being Convex Is the Necessary
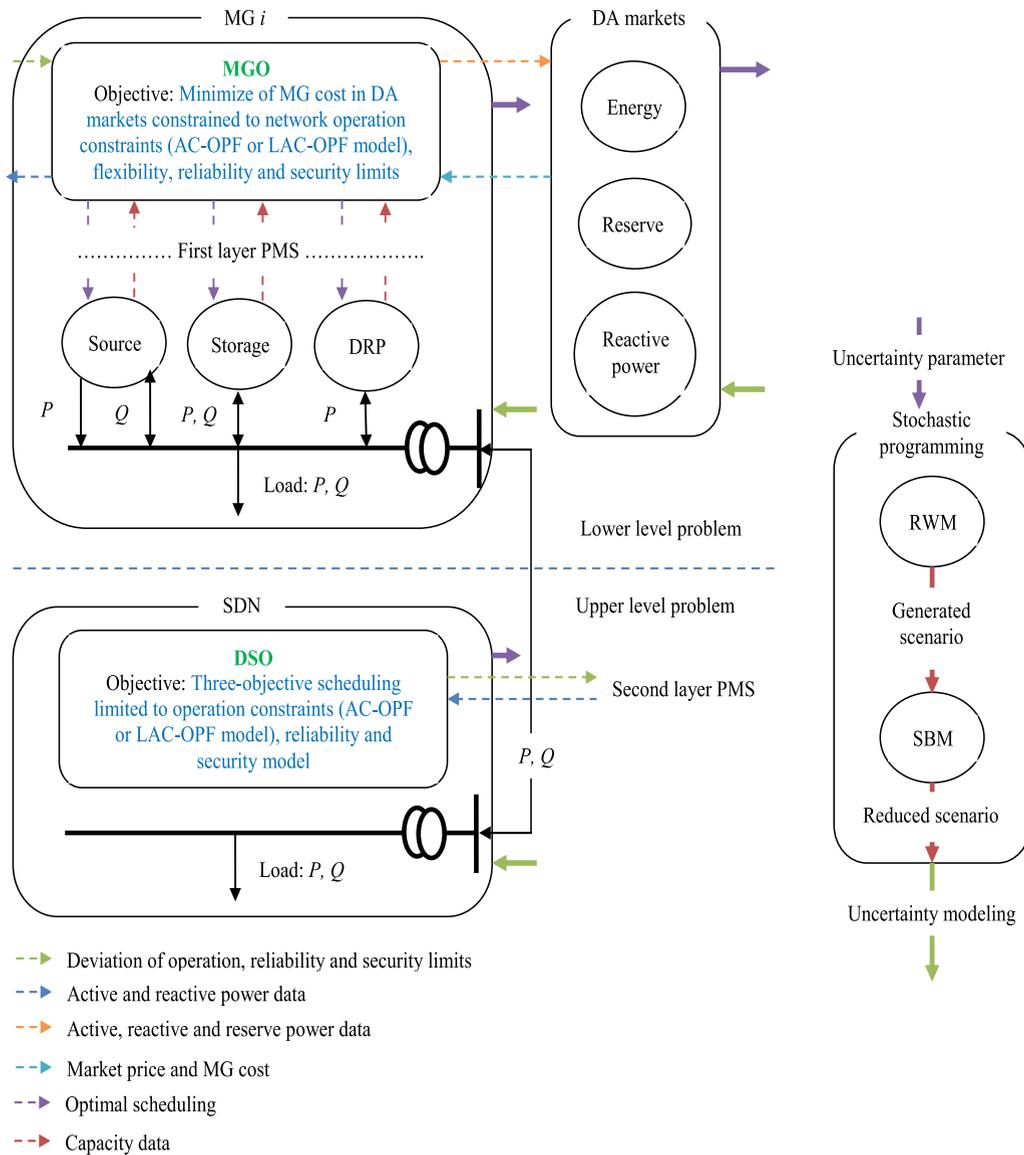
FIGURE 1. The scheme of the scheduling of SDN in the presence of MGs based on two-layer PMS.

Condition to Use the KKT and Other Methods to Transform the Multi-Level Problem Into a Single-Level One. Since the Mentioned Problem Is Subject to AC-OPF Constraints, It Is Non-Convex [15], [16]. To Compensate for This Issue, a Linearized Model Is Used for the Proposed Scheme in Which Linearized AC Optimal Power Flow (LAC-OPF) Constraints Are Used Instead of AC-OPF Equations. For Stochastic Programming Is Incorporated to Model the Uncertainties of Consumption Load, Market Price, Power Generation by Renewables, Energy Demand of EVs, and Availability of Network Equipment. In This Programming, First, the Roulette Wheel Mechanism (RWM) Generates a High Number of Scenarios for the Previously-Mentioned Uncertainties. The Simultaneous Backward Method (SBM) Then Selects a Certain Number of the Generated Scenarios With a Small Distance to Each Other to Apply to the Proposed Problem. The

Contributions of the Present Scheme Are Summarized as Follows:
- Bi-Level Modeling of the Optimal Scheduling of the SDN in the Presence of MGs Based on a Two-Layer Power Management System to Rapidly Process the Data in the DSO;
- Optimal Participation of MGs in the DA Energy, Reactive Power, and Reserve Markets to Achieve Higher Financial Benefit for Sources, Storages, and Responsive Loads; and
- Simultaneous Formulation of Economic, Operation, Reliability, Voltage Security, and Flexibility Indices in the Problem of Optimal Scheduling of the SDN With MMGs.

Note That, Based on Fig. 1, MGO Is Responsible for the Management of MG Power, Meaning That It Receives the Information of Sources and Active Loads and, Based on

That and Technical Limitations of the MG, Makes Decisions for the MG and Its Elements. However, in the SDN, DSO Is Responsible for Power Management. DSO Receives the Information From the MGOs and, Based on That the Technical Limitation of the SDN, Makes Decisions. Since the DSO Is in the Upper-Level Problem, the DSO Is the Chief Program Manager Because MGO Should Manage the Power in the MG in a Way That Technical Limitations and the SDN and MG Are Observed. This Is Achieved by Mutual Cooperation Between MGOs and the DSO. Therefore, It Can Be Stated That the DSO and MGOs Are the Main and Minor Management Elements, Respectively.

In the Remaining, the Bi-Level Stochastic Formulation of the Proposed Scheme Is Presented in Section 2.

Its Single-Level Modeling Is Described in Section 3. Section 4 Evaluates the Numerical Results Obtained for the Problem. In the End, Conclusions Are Provided in Section 5.

II. MODEL OF PROPOSED PROBLEM
A. A BI-LEVEL FORMULATION FOR THE OPERATION OF THE SDN WITH MGs

This Section Describes the Two-Layer Power Management of SDN-Connected MGs Based on MGs' Participation in the DA Energy, Reactive Power, and Reserve Markets. The Coordination Between Sources, Storages, and Responsive Loads Located in the MG and the MGO Is Considered

$$\min F_1 = \vartheta_{EEL} \sum_{\omega \in O_S} \pi_\omega \overbrace{\left\{ \underbrace{\sum_{b \in O_B} \sum_{t \in O_{OH}} P_{DS\,b,t,\omega} + \sum_{t \in O_{OH}} \sum_{i \in O_{MG}} P_{MG\,i,t,\omega}}_{Generation\ Energy} - \underbrace{\sum_{b \in O_B} \sum_{t \in O_{OH}} L_{P\,b,t,\omega}}_{Consumption\ Energy} \right\}}^{EEL}$$

$$+ \vartheta_{EENS} \overbrace{\sum_{\omega \in O_S} \pi_\omega \sum_{b \in O_B} \sum_{t \in O_{OH}} L_{NSb,t,\omega}}^{EENS} - \vartheta_{VSI} \overbrace{\sum_{\omega \in O_S} \pi_\omega \sum_{t \in O_{OH}} WSI_{t,\omega}}^{VSI} \tag{1}$$

Subject To : $L_{NSb,t,\omega} + P_{DS\,b,t,\omega} + \sum_{i \in O_{MG}} A_{MG\,b,i} P_{MG\,i,t,\omega} +$

$$\sum_{j \in O_B} A_{L\,b,j} P_{L\,b,j,t,\omega} = L_{Pb,t,\omega} \quad \forall b, t, \omega \tag{2}$$

$$Q_{DS\,b,t,\omega} + \sum_{i \in O_{MG}} A_{MG\,b,i} Q_{MG\,i,t,\omega}$$

$$+ \sum_{j \in O_B} A_{L\,b,j} Q_{L\,b,j,t,\omega} = L_{Q\,b,t,\omega} \quad \forall b, t, \omega \tag{3}$$

$$P_{L\,b,j,t,\omega} = \left\{ \begin{array}{l} G_{L\,b,j} \sum_{p \in O_P} \left((s_p - V_{\min}) \Delta V_{b,t,\omega,p} - V_{\min}.\Delta V_{j,t,\omega,p} \right) \\ - (V_{\min})^2 B_{L\,b,j} \left(\varphi_{b,t,\omega} - \varphi_{j,t,\omega} \right) \end{array} \right\} \beta_{L\,b,j,\omega} \quad \forall b, j, t, \omega \tag{4}$$

$$Q_{L\,b,j,t,\omega} = \left\{ \begin{array}{l} -B_{L\,b,j} \sum_{p \in O_P} \left((s_p - V_{\min}) \Delta V_{b,t,\omega,p} - V_{\min}.\Delta V_{j,t,\omega,p} \right) \\ - (V_{\min})^2 G_{L\,b,j} \left(\varphi_{b,t,\omega} - \varphi_{j,t,\omega} \right) \end{array} \right\} \beta_{L\,b,j,\omega} \quad \forall b, j, t, \omega \tag{5}$$

$$\varphi_{b,t,\omega} = 0 \ \forall b = \text{Slack bus of SDN}, t, \omega \tag{6}$$

$$P_{DS\,b,t,\omega} \cos(m.\Delta\theta) + Q_{DS\,b,t,\omega} \sin(m.\Delta\theta) \le \bar{S}_{DS\,b} \beta_{DS\,b,\omega} \quad \forall b = \text{Slack bus of SDN}, \omega, m \tag{7}$$

$$P_{L\,b,j,t,\omega} \cos(m.\Delta\theta) + Q_{L\,b,j,t,\omega} \sin(m.\Delta\theta) \le \bar{S}_{L\,b,j} \quad \forall b, j, t, \omega, m \tag{8}$$

$$0 \le \Delta V_{b,t,\omega,p} \le \frac{V_{\max} - V_{\min}}{n_p} \quad \forall b, t, \omega, p \tag{9}$$

$$0 \le L_{NSb,t,\omega} \le L_{Pb,t,\omega} \ \forall b, t, \omega \tag{10}$$

$$WSI_{t,\omega} = (V_{\min})^4 + \sum_{p \in O_P} s'_p \Delta V_{pb-1,t,\omega,p}$$

$$- 4(V_{\min})^2 \left\{ R_{pb-1,pb} P_{L\,pb-1,pb,t,\omega} + X_{pb-1,pb} Q_{L\,pb-1,pb,t,\omega} \right\} \quad \forall t, \omega \tag{11}$$

$$WSI_{t,\omega} \ge WSI^{\min} \quad \forall t, \omega \tag{12}$$

$$P_{MG\,i,t,\omega}, Q_{MG\,i,t,\omega} \in \arg \left\{ \min F_2 = \sum_{\omega \in O_S} \pi_\omega \sum_{t \in O_{OH}} \left\{ \begin{array}{l} \sum_{i \in O_{MG}} \sum_{b \in O_B^{MG}} \beta_{i,b} P_{NR\,i,b,t,\omega} \\ \sum_{i \in O_{MG}} \gamma_{t,\omega} \left(\begin{array}{l} P_{MG\,i,t,\omega} + K_Q Q_{MG\,i,t,\omega} \\ + K_R R_{MG\,i,t,\omega} \end{array} \right) \end{array} \right\} \right\} \tag{13}$$

in the First Layer of PMS, and the Coordination Between MGOs and the DSO Is Assumed in the Second Layer. It Is Assumed That the Main Objectives of DSO Are Achieving Maximum Reliability and Security as Well as Suitable Situation for SDN Operation Indices Such as Minimum Energy Loss and Voltage Drop. Other Assumption, MGO Tries to Obtain Maximum Profit for MG in the Mentioned Markets With Considering Reliability, Security, Operation and Flexibility Constraints. Following This Strategy, Bi-Level Optimization Is Implemented, Where Its Upper Level Refers to the Multi-Criteria Objectives Operation of the SDN in the Presence of MGs to Minimize the Energy Loss, EENS, and Voltage Security Index (VSI) in the Form of a Three-Objective Function Using Pareto Optimization Based on the Sum of Weighted Functions by Satisfying LAC-OPF Constraints and the Reliability and Voltage Security Limitations. The Upper-Level Problem

Deals With the Power Management of the Second Layer. Furthermore, the Formulation of Participation of MGs in the Mentioned Markets in Proportion to the PMS of the First Layer Is Considered in the Lower-Level Problem. Its Objective Function Attempts to Minimize the Difference Between Its Cost and Revenue in the Mentioned Markets. Its Constraints Include LAC-OPF Equations and Reserve, Flexibility, Reliability, and Voltage Security Constraints. Noted That in the SDN Operation Problem, It Needs to Value of Active, Reactive and Reserve Powers of MGs. Hence, the MGs Operation Model Is Used in Lower-Level Formulation, and SDN Optimal Scheduling Is Presented in Upper-Level Model. Thus, the Mathematical Model of the Suggested Scheme Is Presented as Follows. Equations (1)–(13), as shown at the bottom of the previous page. Equations (14)–(27), as shown at the bottom of the page.

Subject To : Constraints (4)-(12) With Adding Index
$$\times \; i \text{ to All Parameters and Variables, and Substituting } DS \text{ to MG}\} \quad \forall i \tag{14}$$

$$L_{NSi,b,t,\omega} + P_{MGi,b,t,\omega} + P_{NRi,b,t,\omega} + P_{Ri,b,t,\omega}$$
$$+ P_{DRi,b,t,\omega} + \left(P_{DISi,b,t,\omega} - P_{CHi,b,t,\omega}\right) + \sum_{j \in O_B^{MG}} A_{Lb,j} P_{Li,b,j,t,\omega} = L_{Pi,b,t,\omega}$$

$$\forall i, b, t, \omega, \; P_{MGi,t,\omega} = P_{MGi,b=slack\ bus\ of\ MG,t,\omega} \tag{15}$$

$$Q_{MGi,b,t,\omega} + Q_{NRi,b,t,\omega} + Q_{Ri,b,t,\omega} + Q_{Ei,b,t,\omega}$$
$$+ \sum_{j \in O_B^{MG}} A_{Lb,j} Q_{Li,b,j,t,\omega} = L_{Qi,b,t,\omega} \quad \forall i, b, t, \omega, \; Q_{MGi,t,\omega} \tag{16}$$
$$= Q_{MGi,b=slack\ bus\ of\ MG,t,\omega}$$

$$- \xi_{i,b} L_{Pi,b,t,\omega} \le P_{DRi,b,t,\omega} \le \xi_{i,b} L_{Pi,b,t,\omega} \quad \forall i, b, t, \omega \tag{17}$$

$$\sum_{t \in O_{OH}} P_{DRi,b,t,\omega} = 0 \quad \forall i, b, \omega \tag{18}$$

$$\underline{E}_{i,b} \le IE_{i,b} + \sum_{t'=1}^{t}\left(\eta_{CH} P_{CHi,b,t',\omega} - \frac{1}{\eta_{DIS}} P_{DISi,b,t',\omega}\right) \le \bar{E}_{i,b} \quad \forall i, b, t, \omega \tag{19}$$

$$0 \le P_{CHi,b,t,\omega} \le \alpha_{CRi,b} \quad \forall i, b, t, \omega \tag{20}$$

$$0 \le P_{DISi,b,t,\omega} \le \alpha_{DRi,b} \quad \forall i, b, t, \omega \tag{21}$$

$$\left(P_{DISi,b,t,\omega} - P_{CHi,b,t,\omega}\right)\cos(m.\Delta\theta)$$
$$+ Q_{Ei,b,t,\omega}\sin(m.\Delta\theta) \le \bar{S}_{Ei,b} \quad \forall i, b, t, \omega, m \tag{22}$$

$$P_{Ri,b,t,\omega}\cos(m.\Delta\theta) + Q_{Ri,b,t,\omega}\sin(m.\Delta\theta) \le \bar{S}_{Ri,b} \quad \forall i, b, t, \omega, m \tag{23}$$

$$P_{NRi,b,t,\omega}\cos(m.\Delta\theta) + Q_{NRi,b,t,\omega}\sin(m.\Delta\theta) \le \bar{S}_{NRi,b} \quad \forall i, b, t, \omega, m \tag{24}$$

$$\left(P_{MGi,b,t,\omega} + R_{MGi,b,t,\omega}\right)\cos(m.\Delta\theta)$$
$$+ Q_{MGi,b,t,\omega}\sin(m.\Delta\theta) \le \bar{S}_{MGi,b}\beta_{MGi,b,\omega} \tag{25}$$
$$\forall R_{MGi,b,t,\omega} \ge 0, i, b = \text{Slack bus of MG}, t, \omega, m$$

$$\overbrace{\sum_{\omega \in O_S} \pi_\omega \sum_{b \in O_B^{MG}} \sum_{t \in O_{OH}} L_{NSi,b,t,\omega}}^{EENS_i} \le EENS^{max} \quad \forall i \tag{26}$$

$$\left. \begin{array}{l} -\Delta F \le P_{MGi,b,t,\omega} - P_{MGi,b,t,\omega'} \le \Delta F \\ \forall i, b = \text{Slack bus of MG}, t, \omega, \omega' \end{array} \right\} \tag{27}$$

1) UPPER LEVEL PROBLEM

The Formulation of the Upper-Level Problem Is Given in (1)-(12). The Objective Function of the Problem as Shown in (1) Is a Three-Objective Function Based on Pareto Optimization Using the Sum of Weighted Functions [22]. In the First Part of This Equation, the Expected Energy Loss (EEL) of the SDN Is Minimized, Which Is Equal to the Difference Between the Energy Generation and Consumption During the Operation Horizon. In the Second Term of Eq. (1), the EENS Caused by the Occurrence of an N - 1 Event Due to an Internal Fault in the Network Equipment Is Minimized. This Energy Similar to the Mentioned Equation Is Equal to the Sum of Load Not-Supplied of the SDN for Internal Faults in Different Equipment During Operation Horizon. In the End, the Third Part of Eq. (1) Minimizes the Symmetry of the VSI [23]. The Worst Security Index (WSI), With a Value Between 0 and 1, Is Employed Here to Analyze Voltage Security. If the Value Is Zero, It Means That Voltage Collapse Has Happened; and a Value of 1 Means That the SDN Is in the No-Load Situation. Moreover, This Index Is Only Calculated for a Weak Bus in Terms of Voltage Magnitude. Such a Bus Can Be Found From Power Flow Results. That Being Said, in Case the Third Part of Eq. (1) Is Maximized, the SDN With High Voltage Security Is Expected to Be Accessible. Thus, a Negative Coefficient Is Used for the Third Part of the Objective Function Given in (1) [23].

As Eq. (1) Has a Three-Objective Form, the Sum of Weighted Coefficients ϑ_{EEL}, ϑ_{EENS}, and ϑ_{VSI} Must Be 1 [22]. To This End, Different Values Are Expected to Be Obtained for EEL, EENS, and VSI Functions for Different Values of These Coefficients, the Depiction of Which in a 3D Coordinate Plane Represents the Pareto Front for the Proposed Scheme [22]. To Find an Optimal Point Equal to the Best Optimal Compromise Solution Among the Mentioned Functions, the Fuzzy Decision-Making Technique (FDT) Is Used in This Paper [24]. In the FDT, First, a Linear Membership Function Is Obtained for EEL, EENS, and VSI Functions for Different Values of Weighted Coefficients. The Membership Value of Each Function Is 1 (0) If the Function's Value Is Smaller (Greater) Than Its Upper (Lower) Limit [24]; Otherwise, the Membership Value of a Function Will Be Equal to the Difference Between the Function With Respect to Its Upper Limit and the Difference Between the Upper and Lower Limits of the Function [24]. The Upper and Lower Limits of EEL, EENS, and VSI Functions Can Be Calculated Using $\vartheta_{EEL} = 1$, $\vartheta_{EENS} = 1$, and $\vartheta_{VSI} = 1$. Then, the Minimum Value Among the Membership Values of EEL, EENS, and VSI Functions Are Determined for Each of the Weighted Coefficients. This Number Is Represented by ϑ in This Paper. Finally, the Point Corresponding to the Best Compromise Solution Among the Mentioned Functions Is Equal to the Maximum Value of ϑ for All Values Selected for Weight Coefficients [24].

Equations (2)-(12) Represent the Constraints of the Upper-Level Problem, Where (2)-(6) Refer to the LAC-PF Constraints in the SDN [1], [7]. These Constraints Indicate Active and Reactive Power Balance at Each Bus, Active and Reactive Power Flow Through the Distribution Line, and Voltage Angle of the Slack Bus. The Real Models of Eqs. (4)-(5) Are Nonlinear Non-Convex in the Form of $P_{Lb,j} = G_{Lb,j}(V_b)^2 - V_b V_j \{G_{Lb,j} \cos(\varphi_b - \varphi_j) + B_{Lb,j} \sin(\varphi_b - \varphi_j)\}$ and $Q_{Lb,j} = -B_{Lb,j}(V_b)^2 + V_b V_j \{B_{Lb,j} \cos(\varphi_b - \varphi_j) - G_{Lb,j} \sin(\varphi_b - \varphi_j)\}$ [6]. However, Since the Difference Between Voltage Angles of Both Near- and Far-End Buses of the Distribution Line in the Distribution Network Is Generally Less Than 6°, the Terms $\cos(\varphi_b - \varphi_j)$ and $\sin(\varphi_b - \varphi_j)$ Can Be Approximated to 1 and $(\varphi_b - \varphi_j)$ [25], [26]. Moreover, Using the Conventional Piecewise Linearization Technique, the Voltage Magnitude Variable Can Be Expressed As, $V_{\min} + \sum_{p \in O_P} \Delta V_p$ Where ΔV Represents Voltage Deviation. By Adopting a Higher Number of Piece-Wises, ΔV Will Take Smaller Values. Following This, the Terms V^2, V^4, $V_b V_j$ and Can Be Written as $(V_{\min})^2 + \sum_{p \in O_P} s_p \Delta V_p$, $(V_{\min})^4 + \sum_{p \in O_P} s'_p \Delta V_p$, and $(V_{\min})^2 + V_{\min} \sum_{p \in O_P} (\Delta V_{b,p} + \Delta V_{j,p})$. Thus, by Neglecting the Terms ΔV^2 and $\Delta V.(\varphi_b - \varphi_j)$ Due to Their Minuscule Values, the Mentioned Nonlinear Terms Can Be Formulated as Eqs. (4) and (5) [25]. The Operation Constraints of the SDN Are Given in (7)-(9), Which Respectively Show the Limitations on the Apparent Power Transferrable Through the SDN's Substation and the Distribution Line and Voltage Deviation Limits on the SDN's Buses [1]. The Real Model of Limits on the Size of Substation and Distribution Line Is a Circular Plane With the Origin in Zero and a Radius of S, $\sqrt{(P)^2 + (Q)^2} \leq S$. A Circular Plane Can Be Approximated by a Regular Polygon in the Form of $P.\cos(m.\Delta\theta) + Q.\sin(m.\Delta\theta) \leq S$ [1], Where If the Number of Sides Is High, the Approximation Will Lead to a Negligible Calculation Error. In This Inequality, m Represents a Side of the Set $O_M = \{1, 2, \ldots, n_m\}$, n_m Is the Number of Sides, and $\Delta\theta$ Denotes the Angle Deviation $(360/n_m)$. In the Real Model of AC-OPF of a Network, the Voltage Magnitude Limit Is Used as $V_{\min} \leq V_{b,t,\omega} \leq V_{\max}$. However, Since the Voltage Deviation Variable Is Used in the LAC-OPF, Eq. (9) Substitutes the Voltage Magnitude Constraint. As Another Remark, It Is Assumed That the SDN Connects to the Upstream Network via the Distribution Substation Placed at the Slack Bus. Thus, Variables P_{DS} and Q_{DS} Will Have Values Only on the Slack Bus. Eventually, Eq. (10) Represents the Reliability Constraint of the SDN, Referring to the Boundary on the Interrupted Load at Consumption Points Due to an N - 1 Event. Equations (11) and (12) Give the Voltage Security Constraint of the SDN, Where the Value of Worst Security Index (WSI) for the Weakest Bus in Terms of Voltage Magnitude Is Calculated by (11). Then, the Limit on This Index Is Provided in (12) [23]. In Other Words, the SDN Should

Always Have a Secure Voltage Margin, Which Is Considered in (12). Note That the Real Model of WSI Is Stated as

$$WSI = (V_{pb-1})^4 - 4(V_{pb-1})^2 \begin{Bmatrix} R_{pb-1,pb}P_{L\,pb-1,pb} + \\ X_{pb-1,pb}Q_{L\,pb-1,pb} \end{Bmatrix} -$$

$$4 \begin{Bmatrix} X_{pb-1,pb}P_{L\,pb-1,pb} - \\ R_{pb-1,pb}Q_{L\,pb-1,pb} \end{Bmatrix}^2,$$

Where the Second and Third Terms Have Very Small Values Compared to the First Term [23]. Hence, Taking This in Mind, Eq. (12) Replaces This Relation. The First Term in (12) Represents the Linear Model of V^4 Based on the Conventional Piecewise Linearization Technique. The Third Term Is Discarded Because of Its Minuscule Value. Also, as the Multiplication of $\sum_{p \in O_P} s_p \Delta V_p$ and $\{R_{pb-1,pb}P_{L\,pb-1,pb} + X_{pb-1,pb}Q_{L\,pb-1,pb}\}$ Gives a Negligible Value, This Term Is Removed From (12).

2) LOWER LEVEL PROBLEM

Equations (13)-(27) Describe the Lower-Level Model of the Problem, Referring to the Participation of MGs in the Energy, Reactive Power, and Reserve Markets. The Objective Function of This Problem, Given by (13), Minimizes the Difference Between the Cost of MGs (including the Operating Cost of Non-Renewables in the First Part of This equation) and Their Expected Revenues in the Mentioned Markets (the Second Term of the equation). Based on the Second Part of (13), in Case Active, Reactive, or Reserve Power Variables Have a Positive Value, MGs Will Produce Revenue in the Mentioned Markets; Otherwise, If the Variables Are Negative, MGs Will Pay a Cost in the Market. Moreover, It Is Considered the Operation Cost of RDGs Is Low, Where It Can Be Ignored [1]. It Is Not Formulated in Equation (13). Constraints (4)-(12) Holds for MGs as Well, so They Are Presented in (14). Active and Reactive Power Balance Constraints in Different Buses of MGs in the Presence of Sources, Storages, and Responsive Loads Will Be as (15) and (16), Respectively. Equation (16) Assumes That Sources and Storages Can Control Reactive Power. Non-Renewable Sources Are Generally Base Generators, so Their Generator Can Control the Reactive Power of These Sources. Renewable Sources and Storages, in General, Are Connected to the Network via Power Electronics. The Reactive Power of These Elements Can Be Controlled by Adopting a Proper Structure for These Converters, Such as Using an IGBT Bridge [21].

Constraints (17)-(18) Present the Formulation of Incentive-Based DRP [27]. In This Model, Consumers Reduce Their Consumption Energy During Peak Hours (corresponding to High Energy prices) in Accordance With the Energy Price Signal and Receive Energy During off-Peak Hours (in Proportion to Low Energy prices). Thus, Constraint (17) Represents the Power Control Limit on Consumers in the Form of a DRP. Constraint (18) Ensures That the Total Energy Reduced During Peak Hours Is Supplied Within the off-Peak Interval. Equations (19)-(22) Refer to the Operation Model of Storages, Respectively Presenting the Limit on Energy Stored

in the Storage Device, Limitations on Charge and Discharge Rates, and the Limit on the Size of Storages Chargers [1]. Concerning Mobile Storages Such as EVs, the Model Given in (19)-(22) Can Be Applied Except That the Number of EVs Differs at Each Scenario and Time. Hence, Subscripts t and ω Are Used for Parameters IE, α_{CR}, α_{DR}, and $\bar{S}_E$. As per [1], [7], $\alpha_{CR}/\alpha_{DR}/\bar{S}_E$ at Hour t Is Equal to the Sum of Charge Rate/Discharge Rate/Charger Size of EVs Connected to the Parking Lot During This Hour. IE at Hour t Is Equal to the Sum of the Initial Energy of EVs Recently Connected to the Parking Lot at Hour t. The Parameter $\bar{E}$ Will Have an ω Subscript Due to the Variable Number of EVs at Each Scenario, and It Is Equal to the Sum of Energy Consumption Required by EVs for Their Travel. In the Operation Model of EVs, the Inequality Term on the Right Side of Constraint (19) Will Be Stated in the Form of Equality. The Constraints on the Model of Operation of Renewables and Non-Renewables Are Provided in (23)-(24), Presenting the Limit on the Size of the Apparent Power of These Sources. The Reserve Power That Always Takes a Positive Value Is Calculated Using (25). In (26), the Limit on EENS for Each MG Is Considered. Note That the Economic Objectives of MGs in the Electricity Market Are Considered as the Objective Function in This Paper; Thereby, Considering the Reliability Constraint of MGs Is Given by a Constraint Similar to (26). In Eq. (27), the Flexibility Limit of MGs Is Presented. The Active Power Generation by RDGs Is Uncertain Because of Prediction Error in Meteorological Conditions Forecast, so It Is Expected That the Active Power of MGs (seen From the Distribution Substation or Slack Bus of This network) Takes Different Values in Different Scenarios. This Will Lead to Unbalance Between the Results of DA and Real-Time Operation [19]. This Is Known as Flexibility Shortage Conditions and, From an Economic Viewpoint, the Cost Imposed by MGs Will Increase as the Penalty of Reduced Flexibility. Hence, to Avoid This Problem, a Constraint Such as (27) Is Used for MGs, Whereby Choosing a Small Value for Flexibility Tolerance (ΔF), the MGs Are Expected to Provide Higher Flexibility, Meaning That the Active Power of MGs Should Be Minimized in Various Scenarios. It Is Worth Noting That the Flexibility Status of MGs in This Paper Is Modified by Active Loads (ALs) and Non-Renewables, and These Elements Are Known as Flexibility Sources.

In the End, It Should Be Noted That Variables P_{NR}, P_{DR}, P_{DIS}, P_{CH}, Q_{NR}, Q_R, and Q_E Are Decision Variables, and Other Variables of the Proposed Problem Are Dependent Variables. In Addition, Reactive Power Limitation of Sources and Storage Devices Is Given in (22)-(24). These Equations Are in the Form of a Circular Plane in the PQ Coordinates and Is Known as Capability Curve of the Mentioned Elements. Also, the Above Papers Are Considered in [28]–[30].

B. STOCHASTIC PROGRAMMING OF UNCERTAINTIES

in the Problem Described by (1)-(27), Parameters of Load (L_P, L_Q), Renewable Power (P_R), Energy Price (γ), Charge and Discharge Rates (α_{CR}, α_{DR}), Initial Energy and Charger

Size of EVs (IE, $\bar{S}_E$), Consumption Energy by EVs ($\bar{E}$), Availability of SDN Equipment and MGs (β_{DS}, β_{MG}, β_L) Are Uncertainty Parameters. To Address This, Stochastic Programming Based on the RWM and SBM Is Utilized to Model These Uncertainty Parameters. The RWM Generates a High Number of Scenarios, Where the First 9 Uncertainty Parameters in Each Scenario Are Determined Based on Their Mean and Standard Deviation. However, the Values of the Three Last Uncertainties Are Found Based on the Force Outage Rate (FOR) of Network Equipment and MGs [27], [31], [32]. Moreover, the Probability of the Selected Values for Load and Energy Price Parameters Is Calculated in Each Scenario Using the Normal Probability Distribution Function (PDF) [1]. The Probability of Values of Renewable Power for Wind and Photovoltaic Systems Are Specified Based on Weibull and Beta PDFs, Respectively [1]. The Probability of Values for Parameters of EVs Is Found Using Rayleigh PDF [27], and It for the Three Last Uncertainties Calculates Based on Bernoulli PDF [24]. The Probability of Occurrence of an Event in Each Scenario (π_0) Is Equal to the Multiplication of the Probabilities of Uncertainty Parameters in That Scenario. In the Next Step, the SBM Chooses a Small Number of the Generated Scenarios and Applied Them to the Proposed Problem. It Should Be Noted That Scenarios With a Small Distance From Each Other Are Selected in This Method. The Probability of New Scenario (π) Is Equal to Rate of Its π_0 and Sum of π_0 for All Scenarios Obtained by SBM. The Detailed Information About the Formulation of the Mentioned Method Is Accessible in [33].

III. SINGLE-LEVEL MODEL OF THE PROPOSED PROBLEM

Reaching a Single-Level Model Is a Necessity to Find an Optimal Solution for the Problem (1)-(27) by Using TRaditional Solvers [27]. Since That This Problem Includes Linear Formulation, Thus, It Includes a Convex Model. Hence, the KKT Is Employed as Follows.

The Model of the Problem That Early Has Been Discussed Has a General Structure of the Problem (28)-(32). The Upper- and Lower-Level Problems Are Described by (28)-(29) and (30)-(32), Respectively. The Vector for Variables of the Upper or Lower Level Problem Is Denoted by x (y). Parameters ρ and μ Are the Lagrangian Multipliers.

$$\min F_1 = a^T x + b^T y \tag{28}$$

$$\text{Subject To: } c_1.x + d_1 y (\leq / = / \geq) e_1 \tag{29}$$

$$y \in \arg \left\{ \min \quad F_2 = f^T y \right. \tag{30}$$

$$\text{Subject To: } g_1 y = h_1 : \rho \tag{31}$$

$$\left. g_2 y \leq h_2 : \mu \right\} \tag{32}$$

We Need to Use the Constrained Found Using the KKT of the Lower-Level Problem in the Upper-Level Problem, Aiming to Find the Single-Objective Model of the Problem Being Discussed [27]. One Solution Is to Find the Lagrangian Function (L) of the Lower Level Problem (33). The Objective Function and Penalty Functions Related to the Problem Constraints Are Put Together to Find the Lagrangian Function.

The Penalty Function for Constraints $a \leq b$ and $a = b$ Are Given by $\mu.\max(0, a - b)$ and $\rho.(b - a)$, Respectively [27].

$$L = F_2 + \rho.(h_1 - g_1 y) + \mu.\max(0, g_2 y - h_2) \tag{33}$$

The Constraints Found by KKT Are in Proportion to Making Derivative of the Lagrangian Function Equal to Zero by Differentiating It With Respect to Its Variables (y, μ, and ρ) [27]. As a Result, the Single-Level Formulation of the Problem (28)-(32) Are According to (34)-(39). In the Newly Formed Problem, Eqs. (34), and (35) Equivalent to (28)-(29) Describe the Upper-Level Problem. Equation (36) Is Found by Making of the Differentiation of the Lagrange Function Zero With Respect to the Primal Variable of the Lower-Level Problem (y). Equation (37) Is Formed Through $\frac{\partial L}{\partial \rho} = 0$, Which Will Be Same as Constraint (31). The Result of $\frac{\partial L}{\partial \mu} = 0$ (μ Is the Lagrange Multiplier of an Inequality constraint) Is Constrained by Two Conditions as Eq. (38), Where (32) Is Reached According to Its First Condition, and $\mu.(g_2 y - h_2) = 0$ Is Extracted as per the Second Condition. This Constraint Is Nonlinear. To Express Its Linear Form, $-M.z \leq \mu \leq M.z$ and $-M.(1-z) \leq (g_2 y - h_2) \leq M.(1-z)$ Are Used in $\mu.(g_2 y - h_2) = 0$, Where M Represents a Large Fixed Number Like 10^6 and z Denotes a Binary Variable [27]. Equation (39) Provides the Range of Lagrange Multipliers.

$$\min F_1 = a^T x + b^T y \tag{34}$$

$$\text{Subject To: Constraint (29)} \tag{35}$$

$$\frac{\partial L}{\partial y} = 0 \Rightarrow g_1 \rho + g_2 \mu = f \tag{36}$$

$$\frac{\partial L}{\partial \rho} = 0 \Rightarrow \text{Constraint}(31) \tag{37}$$

$$\frac{\partial L}{\partial \mu} = 0$$

$$\Rightarrow \begin{cases} \text{Constraint (32)} & \forall \text{First condition} \\ \mu.(g_2 y - h_2) = 0 & \forall \text{Second condition} \end{cases} \tag{38}$$

$$\rho \in (-\infty, +\infty), \ \mu \in [0, +\infty) \tag{39}$$

Finally, the Flowchart of the Problem Solving Is as Fig. 2.

IV. NUMERICAL RESULTS

A. CASE STUDIES

The Proposed Scheme Is Implemented on a 33-Bus Radial SDN [34]–[36] With Three MG1, MG2, and MG3 Microgrids, as Shown in Fig. 3. The Peak Load Data and Specifications of Distribution Lines and Substation of the SDN Are Reported in [13], and This Data for MGs Is Given in [16]. Bus 1 for the SDN Is the Slack Bus, and Buses 10, 20, and 26 Are the Slack Buses for the First to Third MGs, as Depicted in Fig. 3. The Limitation on the Voltage Magnitude for the Mentioned Networks Is [0.9, 1.1] p.u. There Are Renewable Sources Such as Wind and Photovoltaic Systems and Non-Renewable Sources Such as Diesel Generators in the MG, the Data of Which Can Be Found in [16]. Ref. [16] Does Not Discuss the Charger Size of Batteries, but We Set It
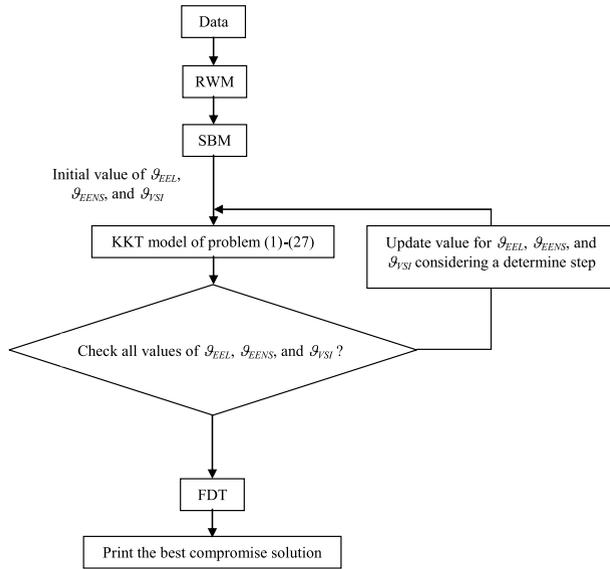
FIGURE 2. Flowchart of the solving of proposed problem.

FIGURE 3. Case study of system [34].

FIGURE 4. Daily curve of, a) RDG power rate and load factor, b) EVs penetration rate [1].

TABLE 2. Specifications of EV [6], [7].

Battery capacity ($\bar{E}$) in kWh	BC≤8	8≤BC≤15	BC≥15
$IE/\bar{E}$	0	0.15	0.25
Charger capacity (kVA)	3.3	4.6	6.6
Charge (Discharge) rate (kW)	2.5	4	6
EVs in each group (%)	20	60	20

to 50% of the Battery Size in This Paper. The Authors in [16] Also Do Not Provide the Data of EVs Parking Lot, but the Present Study Assumes That There Are Renewable Sources on the Buses of MGs and the Capacity of EVs Parking Lot Is 300 Vehicles. Specifications of EVs, Including Charge and Discharge Rates, Charger Size, etc. Are Expressed in Table 2 [6, 7]. In MGs, It Is Assumed That Consumers Participate in the DRP With a Rate of 30% [27]. Energy Price for the DA Energy Market During 1:00-7:00, 8:00-16:00, 23:00-00:00, and 17:00-22:00 Is Set 16 $/MWh, 24 $/MWh, and 30 $/MWh, Respectively [7]. The Term K_Q Is Set at 0.08 as per [7], and K_R Is Set 1. The Hourly Data of Load (power Generation by Renewable source) Is Equal to the Multiplication of Peak Load (size of source) and Load Factor (Power Rate). The Number of EVs Connected to the Parking Lot at Each Hour Is Equal to the Total Number of EVs Connectable to the Parking Lot and the Penetration Rate of EVs. The Daily Load Factor Curve, the Power Rate of Renewable Sources, and the Penetration Rate of EVs in the Parking Lot Are Depicted in Fig. 4 [1]. The Value of WSI^{min} Is 0.8 [23]. The Weak Buses in Terms of Voltage Magnitude Obtained Based on Power Flow Studies in the SDN and the First to Third MGs Are Buses 18, 14, 12, and 14, Respectively. The RWM Generates 2000 Scenarios. The SBM Then Applies 80 of the Scenarios to the Problem. The s.T of Uncertainties of Load, Energy Price, Renewable Power, and Energy Demand of EVs Is Set 10%. The for Value for Network Equipment and Elements of MGs Is Considered 1%.

V. RESULTS

the Proposed Scheme Is Simulated in GAMS Optimization Software in Accordance With the Data Provided in Subsection IV.A. The CPLEX Solver Is Then Used to Solve the Problem [37]–[40]. Five Pieces Are Considered for the

Conventional Piecewise Linearization Technique. Also, the Circular Plane Is Approximated by a Regular 45-Gon [25]. Based on the Results Obtained in [25], It Is Observed That the Computational Error of the Linear Approximation Model Used for the AC-OPF Problem, Described by (1)-(10), Is 2% and 0.5% for Power and Voltage Variables in Comparison to the Original (Nonlinear) AC-OPF Problem. This Error Can Be Neglected Due to Its Low Computational Time [25].

1) EVALUATION OF THE BEST COMPROMISE SOLUTION

Table 3 Reports the Pareto Front's Results Related to the Proposed Scheme for Weighted Coefficients ϑ_{EEL}, ϑ_{EENS}, and ϑ_{VSI} With Values 0, 0.33, 0.5, and 1. The Cases With $\vartheta_{EEL} = 1$, $\vartheta_{EENS} = 1$, and $\vartheta_{VSI} = 1$ in This Table Calculate the Minimum Values of EEL and EENS Functions and the Maximum

Value of the VSI in the SDN. The Minimum Values of EEL and EENS Are Respectively 1.811 MWh and 1.673 MWh, and Maximum Value of VSI Is 22.35. Note That, in Eq. (1), the Term *min* Has Been Used for the Symmetry of VSI. On That Account, Eq. (1) Attempts to Maximize the VSI. In These Three Cases, We Can Obtain the Maximum Values of EEL and EENS and the Minimum Value of the VSI. The Maximum Value of EEL Is 1.957 MWh, Which Is Obtained When EENS Is Minimized in Eq. (1). The Maximum Value of EENS Is Found 4.312 MWh, Which Was Calculated When the Symmetry of VSI Is Minimized. The Minimum Value of VSI (That Is 20.09) Is Extracted When the EENS Is Minimized. So, the Ranges of Changes of These Functions Are 0.146 (1.957 - 1.811) MWh, 2.639 (4.312 - 1.673) MWh, and 2.26 (22.35 - 20.09). Furthermore, It Is Observed in Table 3 That the Direction of Changes of the Mentioned Functions Is Not the Same. For Instance, the Reduction in EENS Is Commensurate With the Increase in EEL Because to Minimize EENS, High Amounts of Active Power Need to Be Supplied by Sources, Storages, and Responsive Loads Into the Network; Although This May Swell Power Loss of Distribution Lines and Thus Increase the Expected Energy Loss.

Table 4 Lists the Best Solutions Compromised Among EEL, EENS, and VSI Functions When the Pareto Optimization Technique Is Based on Using the Sum of Weighted Functions, Normalized Objective Function [6], and ε-Constraint Methods [24]. Referring to This Table, the Values of EEL, EENS, and VSI Functions at the Best Compromise Solution Point Are 1.851 MWh, 2.084 MWh, and 22.03, Respectively, That Are Proportional to the Case With $\vartheta_{EEL} = 0.1$, $\vartheta_{EENS} = 0.0$, and $\vartheta_{VSI} = 0.81$. The Values of the Mentioned Functions Are Close to Their Minimum, Minimum, and Maximum Value, Where EEL, in This Case, Is 27.4% ((1.851 - 1.811)/0.146) Close to Its Minimum Value. EENS Is 15.6% Distant From Its Minimum, and the Distance Between the VSI and Its Maximum Value Is 14.2%. Table 4 Also Provides the Results Obtained by Applying the Sum of Weighted Functions Using the Normalized Objective Function and ε-Constraint Methods for the Proposed Scheme. In the Normalized Objective Function Method, the Values of Weighted Coefficients ϑ_{EEL}, ϑ_{EENS}, and ϑ_{VSI} Are Such Determined That the Ranges of Changes of Terms $\vartheta_{EEL} \times$ EEL, $\vartheta_{EENS} \times$ EENS, and $\vartheta_{VSI} \times$ VSI Are the Same [6]. Now, by Choosing $\vartheta_{EENS} = 1$, the Values of ϑ_{EENS} and ϑ_{VSI} Are Found 18.075 (2.639/0.146) and 1.168 (2.639/2.26). It Is Seen in This Method That Higher Values Are Obtained for the Mentioned Functions Compared to the Sum of the Weighted Functions Method. This Holds Also When Comparing ε-Constraint and the Sum of Weighted Functions Method. As a Result, the Method Adopted in This Paper Provides Superior Capabilities to Other Methods in the Pareto Optimization Technique in Improving the Optimal Solution of the Proposed Scheme. Eventually, Based on Table 4, the Computational Time of the Sum of Weighted Functions and ε-Constraint Methods Is About 16-17 s, While It Is 9.7 in the

TABLE 3. Pareto front of the proposed scheme.

ϑ_{EEL}	ϑ_{EENS}	ϑ_{VSI}	EEL (MWh)	EENS (MWh)	VSI (%)
1	0	0	1.811	4.121	20.66
0	1	0	1.957	1.673	20.09
0	0	1	1.906	4.312	22.35
0.5	0.5	0	1.884	2.735	20.37
0.5	0	0.5	1.868	4.083	21.76
0	0.5	0.5	1.915	3.052	21.11
0.33	0.33	0.33	1.901	3.142	21.09

TABLE 4. The best compromise solution between function of EEL, EENS and VSI in 33-bus SDN.

Method	ϑ_{EEL}	ϑ_{EENS}	ϑ_{VSI}	EEL (MWh)	EENS (MWh)	VSI (%)	Calculation time (s)
Sum of weighted functions	0.15	0.04	0.81	1.851	2.084	22.03	16.2
Normalized function	18.075	1	1.168	1.863	2.551	21.87	9.7
ε-constrain				1.853	2.114	21.98	17.1

Normalized Objective Function Method Because the Former Two Methods Require to Extract the Pareto Front, Which Is Not the Case in the Latter Method.

2) EVALUATION OF MGs' ECONOMIC STATUS

Fig. 5 Illustrates the Graph of Expected Profit for the First to Third MGs in Terms of Changes in Flexibility Tolerance (ΔF) and Maximum EENS ($EENS^{max}$). Fig. 5(A) Shows the Profit-Flexibility Tolerance Curve for MGs for $EENS^{max} = 1$. According to This Figure, Increasing ΔF Escalates the Expected Profit of MGs in the Energy, Reactive Power, and Reserve Market Because, Under These Conditions, the Importance of Flexibility Index Decreases in the Proposed Scheme; Thus, the Operation of Non-Renewable Sources, Storages, and Responsive Loads Will Be Such That Their Operating Cost Is Minimized so That Higher Profit Is Produced for MGs as per (13). These Conditions Continue Until $\Delta F = 0.06$ mW. For $\Delta F > 0.06$ mW, the Expected Profit of MGs Is Fixed. Fig. 5(b) Depicts the $EENS^{max}$ - Profit Curve for MGs. As $EENS^{max}$ Increases, so Does the Expected Profit of MGs, as Given in Fig. 5(b), Because the Increase in $EENS^{max}$ Is Following the Increase in the Solution Space of the Problem Based on the Constraint (26), Thus Leading to Increased Profit. For $EENS^{max} > 8$ MWh, the Profit Will Have a Fixed Value. However, for $EENS^{max} < 1$ MWh, the Proposed Scheme Cannot Achieve the Optimal Solution. So,

TABLE 5. Expected MGs profit in different cases.

	Case	ΔF (MW)	$EENS^{max}$ (MWh)	Profit ($)
I	MG1	0	1	206
	MG2	0	1	629
	MG3	0	1	193
II	MG1	0.0221	3.12	261
	MG2	0.0219	3.10	739
	MG3	0.0222	3.12	242

the Results Concerning This Range of $EENS^{max}$ Are Not Depicted in Fig. 5(b).

Table 5 Investigates the Economic Situation of MGs for Two Case Studies:

- **Case I**: Implementing the Proposed Scheme, (1)-(27), With Respect to the Compromise Point $\vartheta_{EEL} = 0.15$, $\vartheta_{EENS} = 0.04$, and $\vartheta_{VSI} = 0.8$ and High Flexibility and Reliability Status for MGs ($EENS^{max} = 1$ MWh, $\Delta F = 0$);
- **Case II**: Implementing the Proposed Scheme, (1)-(27), With Respect to the Compromise Point $\vartheta_{EEL} = 0.15$, $\vartheta_{EENS} = 0.04$, and $\vartheta_{VSI} = 0.8$ and the Best Compromise Solution Among Economic, Reliability, and Flexibility Status of MGs.

in Case II, First, the Expected Profit of MGs (symmetry of Eq. (13)), EENS of MGs (left Side of Constraint (26)), and Flexibility of MGs (max $\left(\left| P_{MG\,i,b,t,\omega} - P_{MG\,i,b,t,\omega'} \right| , \forall i, b, t, \omega, \omega' \right)$) Is Calculated for Different Values of ΔF and $EENS^{max}$. Then, Using the FDT, the Best Compromise Solution Among the Functions Is Obtained. As per Table 5, the Expected Profit of MGs in Case I Is Less Than in Case II; Nevertheless, This Case Ensures High Reliability and Flexibility (smaller ΔF and $EENS^{max}$) for MGs. In Case II, as the Values of ΔF and $EENS^{max}$ Increase by 0.022 mW and 3.12 MWh, a Compromised Situation Can Be Found for Economic, Reliability, and Flexibility Indices of MGs Because, in These Circumstances, the Expected Profit of MGs Is High and Flexibility Tolerance and $EENS^{max}$ Have Smaller Values.

3) EVALUATION OF MGs' OPERATION

Fig. 6 Shows the Daily Expected Curve of MGs in the Energy, Reactive Power, and Reserve Market for Case Study II. According to Fig. 6(A), by Proper Management of Sources, Storages, and Responsive Loads, MGs Inject Active Power Into the SDN During All Operation Hours and Gain Financial Benefit From the Energy Market. They, However, Inject Lower Active Power Into the SDN During the Early Hours of Operation (1:00-4:00) and Last Hours of Energy Scheduling (18;00-00:00) Compared to Other Hours. The Reason Is That, Based on the Data Provided in Subsection IV.A, the Energy Price During 1:00-4:00 Is the Least Compared to That During Other Intervals, and the Fuel Price of Non-Renewable Sources in These Hours (20 $/MWh) Is Higher Than Energy Price (16 $/MWh). Therefore, to Minimize MGs' Cost, Eq. (13), EVs, Batteries, and Responsive Loads Are Energy

Consumers and Non-Renewable Sources Inject Lower Power Into the MGs During These Intervals. From 18:00 to 00:00, the Passive Load of the Network Is High, Meaning That the Network Is Heavily Loaded. Thereby, MGs Are Less Capable of Injecting Active Power Into the SDN During These Periods. Another Remark Is That Renewable Sources Cannot Produce High Amounts of Active Power During 1:00-4:00 and 18:00-00:00, as Shown in Fig. 3, and Photovoltaics Are Switched off in These Hours. Due to High Power Generation by Sources and Reduced Energy Consumption by EVs, Batteries, and Responsive Loads From 5:00 to 17:00, MGs Can Inject Higher Active Power Into the SDN in Comparison to Other Hours.

The Daily Expected Reactive Power Curve of MGs for Case II Is Depicted in Fig. 6(b). Based on This Figure, MGs Are Reactive Power Generators in the Operation Horizon Because, as per (16), MGs Receive Reactive Power From Renewable and Non-Renewable Sources and Storages. Since the Number of Reactive Sources and Their Size in MGs Is High According to Subsection IV.A, They Act as Reactive Power Generators in the SDN. Note That During 1:00-6:00, MGs Produce Higher Amounts of Reactive Power Because, Based on Fig. 6(A), Storages and Responsive Loads Are in the Charging Status. Hence, to Prevent Drastic Voltage Drop During These Hours, the Sources Inject Higher Reactive Power Into the MG. From 7:00-00:00, the Reactive Power of MGs Is Low Given That Sources Allocate a Higher Share of Their Capacity to Generate Active Power During These Intervals, as Illustrated in Fig. 6(A). Accordingly, the Capacity of Reactive Power Generation by Sources Has Decreased in These Conditions. The Daily Expected Reserve Power Curve of MGs Is Shown in Fig. 6(c), According to Which MGs Can Meet the Reserve During 5:00-18:00 Considering That Sources Can Produce Higher Amounts of Energy in This Interval, as Given in Fig. 6(c) and They Allocate a Small Part of Their Capacity to Generate Reactive Power. On That Account, Referring to (25) and the Data of Subsection IV.A, the Capacity of MGs Is High and They Can Play a Role in Supplying the Reserve During These Hours. In the Rest of the Hours, the Consumption Load Is Large and Considerable Amounts of Sources, Storages, and Responsive Loads (Only During Peak Hours) Are Allocated to Supply the Demand. Also, to Hinder Extreme Voltage Drop in These Conditions, a Share of the Capacity of Sources and Storages Needs to Be Allocated to Reactive Power Generation. Consequently, the Capacity of MGs Is Low Within This Period and MGs Will Have No Role in Supplying the Reserve During 1:00-4:00 and 19:00-00:00 as Presented in Fig. 6(c).

4) EVALUATION OF TECHNICAL STATUS OF NETWORKS

Table 6 Analyzes the Values of Operation Indices Including EEL, Maximum Voltage Drop (MVD), Maximum Overvoltage (MOV), Reliability Index (EENS), Voltage Security Index (VSI), and Flexibility Index (ΔF) for MGs and the SDN for Two Case Studies. One of the Case Studies Is Case II and the Other (Case III) Refers to Power Flow Studies
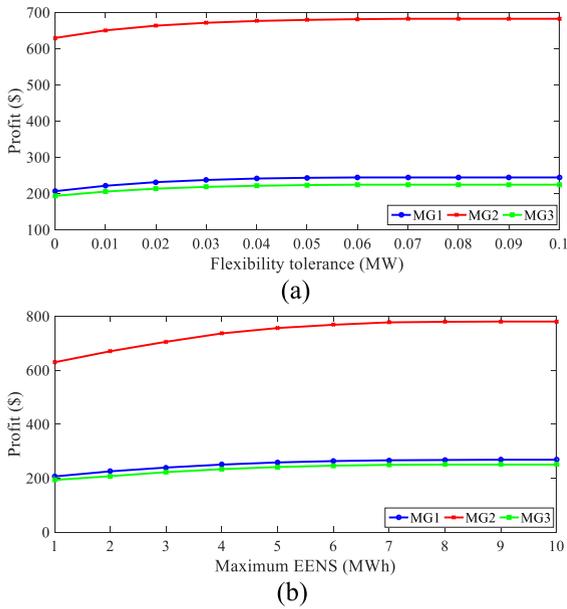
FIGURE 5. Expected profit curve of MGs in, (a) Flexibility tolerance ($EENS^{max}$ = 1 MWh), (b) $EENS^{max}$ ($\Delta F = 0$).
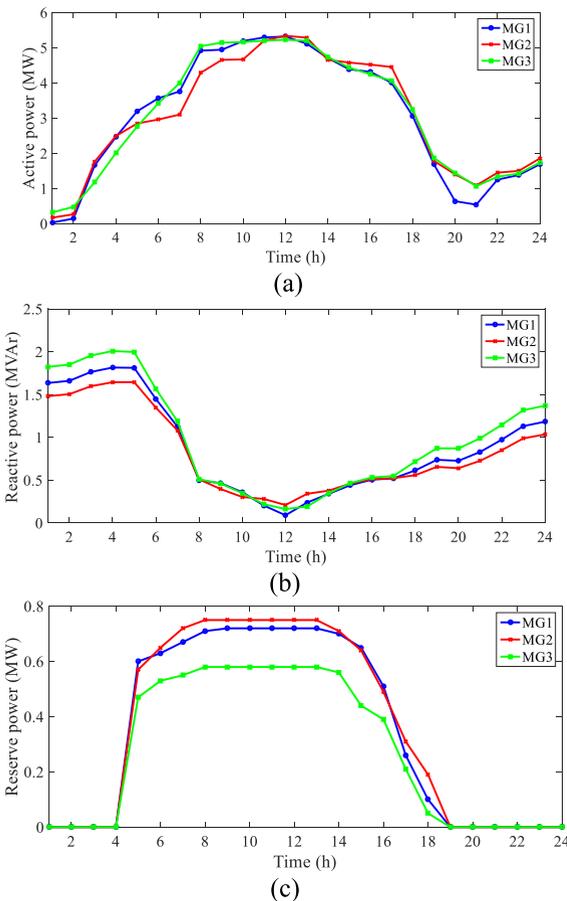
FIGURE 6. Expected daily curve Of, (a) Active power, (b) Reactive power, (c) Reserve power for different MGs.

on the Mentioned Networks. Based on Table 6, by Proper Management of Sources, Storages, and Responsive Loads

TABLE 6. Value of technical indices in SDN and MGs.

	Case	EEL (MWh)	MVD (p.u)	MOV (p.u)	EENS (MWh)	VSI (%)	ΔF (MW)
III	MG1	6.581	0.102	0	31.3	19.41	-
	MG2	5.345	0.143	0	29.8	19.34	-
	MG3	1.819	0.091	0	24.4	19.55	-
	SDN	2.461	0.087	0	26.1	19.78	-
II	MG1	4.242	0.068	0.0151	3.12	21.93	0.0221
	MG2	3.479	0.061	0.0147	3.10	21.88	0.0219
	MG3	1.267	0.045	0.0123	3.12	21.96	0.0222
	SDN	1.851	0.058	0.0126	2.084	22.03	-

According to the Proposed Strategy, (1)-(27), the Proposed Scheme (Case II) Can Enhance All Technical Indices of the Networks Compared to Case III. The Proposed Scheme Helps MGs to Take Higher Flexibility Capability With a Maximum Tolerance of 0.022 mW. For Flexibility of 100%, ΔF Is Zero. The Proposed Scheme in Case II Obtains Conditions Close to This Point for MGs, Meaning That the Flexibility of MGs Is High. Moreover, Voltage Security of Networks, Which Was Around 19.3-19.8 in Case III, Has Enhanced in Case II. This Index for the Mentioned Networks Has Increased to 21.88-22.03 in This Case. In Case III, the Networks Have High EENS (Greater Than 24 MWh) in Case an N - 1 Event Occurs; While It DegRades to Less Than 3.2 MWh in Case II. Concerning the Operation Index, the Proposed Scheme With MOV Between 0.012-0.015 p.u. (less Than the Permissible Limit, 0.1 (1.1 - 1) p.u.) Has Succeeded to Decrease the MVD to 0.068 p.u. In Different Networks. In the End, the Energy Loss of the First to Third MGs and the SDN Has Decreased by Approximately 35.5% ((6.581-4.242)/6.581), 34.9%, 30.3%, and 24.8% in Case II Compared to Case III.

VI. CONCLUSION

This Paper Presented the Two-Layer Power Management of MGs in the SDN While Considering the Participation of MGs in the Day-Ahead Energy, Reactive Power, and Reserve Market. The Proposed Scheme Was Presented as a Bi-Level Problem, the Upper Level of Which Deals With the Optimal Scheduling of the SDN Based on the Second Layer's PMS (coordination Between MGs' Operators and the DSO) Considering the Objective Functions of Minimizing Energy Loss, EENS, and Symmetry of Voltage Security Index. The Problem Was Formulated in the Form of Pareto Optimization Based on the Sum of Weighted Functions. This Problem Was Constrained to LAC-OPF Equations and Limitations of Reliability and Voltage Security. The Lower-Level Problem, on the Other Hand, Addressed Modeling the Participation of MGs in the Mentioned Markets Based on the Second Layer's PMS (coordination Between Sources, Storages, and Responsive Loads and MG operators); the Objective Function of Which Aims to Minimize the Difference Between the Expected Cost of Non-Renewable Sources and the Expected Revenue of MGs From the Markets. This Problem Is Also Subject to the Model of MG and Limitations of Reliability, Operation, Security, and Flexibility. The KKT Method

Obtained a Single-Level Problem, and Stochastic Programming Was Used to Model the Uncertainties of Load, Energy Price, Renewable Power, the Energy Demand of Mobile Storages, and Availability of Network Equipment. In the End, by Evaluating the Numerical Results It Was Observed That the Sum of Weighted Functions Method in the Proposed Multi-Objective Problem Can Provide a Compromised Solution, for Which the Values of Energy Loss, EENS, and Symmetry of VSI Are Close to Their Corresponding Minimum Values. The Energy Loss in the Compromise Point Is Almost 27.4% Away From Its Minimum Point. This Amount for the Expected Energy Not-Supplied Is About 15.6% and It Is About 14.2% for the Symmetry of VSI. Moreover, With Proper Management of Sources, Storages, and Responsive Loads Following the Suggested Strategy and Considering the Best Compromise Status Among Economic, Flexibility, and Reliability Indices in MGs, the New Scheme Gives Maximum Flexibility Tolerance of 0.022 mW Compared to Power Flow Studies. In Comparison to Power Flow Studies, the Proposed Scheme Also Helps DegRade High Values of EENS From Above 24 MWh Down to 3.2 MWh, Reduce VSI to Around 22, Reduce MVD to Under 0.068 p.u., and Energy Loss by About 30%. Furthermore, the Profit Obtained for MGs From the Mentioned Markets Is Dependent on the Reliability and Flexibility Limitations of MGs. As the Importance of These Indices in the Network (relaxation of the Problem From These constraints) Reduces, the Profit of MGs in the Mentioned Markets Increases.

REFERENCES

[1] S. A. F. Asl, L. Bagherzadeh, S. Pirouzi, M. Norouzi, and M. Lehtonen, "A new two-layer model for energy management in the smart distribution network containing flexi-renewable virtual power plant," *Electr. Power Syst. Res.*, vol. 194, May 2021, Art. no. 107085.

[2] A. Ouammi, "Model predictive control for optimal energy management of connected cluster of microgrids with net zero energy multi-greenhouses," *Energy*, vol. 234, pp. 34–45, Nov. 2021.

[3] M. Bollen, "The smart grid: Adapting the power system to new challenges," in *The Smart Grid: Adapting the Power System to New Challenges*. San Rafael, CA, USA: Morgan & Claypool, 2011.

[4] B. Tan and H. Chen, "Multi-objective energy management of multiple microgrids under random electric vehicle charging," *Energy*, vol. 208, pp. 23–35, Oct. 2020.

[5] M. Hu, Y.-W. Wang, J.-W. Xiao, and X. Lin, "Multi-energy management with hierarchical distributed multi-scale strategy for pelagic islanded microgrid clusters," *Energy*, vol. 185, pp. 910–921, Oct. 2019.

[6] S. Pirouzi, M. A. Latify, and G. R. Yousefi, "Conjugate active and reactive power management in a smart distribution network through electric vehicles: A mixed integer-linear programming model," *Sustain. Energy, Grids Netw.*, vol. 22, Jun. 2020, Art. no. 100344.

[7] H. Kiani, K. Hesami, A. Azarhooshang, S. Pirouzi, and S. Safaee, "Adaptive robust operation of the active distribution network including renewable and flexible sources," *Sustain. Energy, Grids Netw.*, vol. 26, Jun. 2021, Art. no. 100476.

[8] R. Homayoun, B. Bahmani-Firouzi, and T. Niknam, "Multi-objective operation of distributed generations and thermal blocks in microgrids based on energy management system," *IET Gener., Transmiss. Distrib.*, vol. 15, no. 9, pp. 1451–1462, May 2021.

[9] Y. Cao, W. Wei, L. Wu, S. Mei, M. Shahidehpour, and Z. Li, "Decentralized operation of interdependent power distribution network and district heating network: A market-driven approach," *IEEE Trans. Smart Grid*, vol. 10, no. 5, pp. 5374–5385, Sep. 2019.

[10] S. Hu, Y. Xiang, J. Liu, C. Gu, X. Zhang, Y. Tian, Z. Liu, and J. Xiong, "Agent-based coordinated operation strategy for active distribution network with distributed energy resources," *IEEE Trans. Ind. Appl.*, vol. 55, no. 4, pp. 3310–3320, Jul./Aug. 2019.

[11] S. Parhizi, A. Khodaei, and M. Shahidehpour, "Market-based versus price-based microgrid optimal scheduling," *IEEE Trans. Smart Grid*, vol. 9, no. 2, pp. 615–623, Mar. 2018.

[12] Y. Li, Z. Yang, G. Li, D. Zhao, and W. Tian, "Optimal scheduling of an isolated microgrid with battery storage considering load and renewable generation uncertainties," *IEEE Trans. Ind. Electron.*, vol. 66, no. 2, pp. 1565–1575, Feb. 2019.

[13] R. Lahon, C. P. Gupta, and E. Fernandez, "Optimal power scheduling of cooperative microgrids in electricity market environment," *IEEE Trans. Ind. Informat.*, vol. 15, no. 7, pp. 4152–4163, Jul. 2019.

[14] M. Hemmati, B. Mohammadi-Ivatloo, M. Abapour, and A. Anvari-Moghaddam, "Optimal chance-constrained scheduling of reconfigurable microgrids considering islanding operation constraints," *IEEE Syst. J.*, vol. 14, no. 4, pp. 5340–5349, Dec. 2020.

[15] E. Faraji, A. R. Abbasi, S. Nejatian, M. Zadehbagheri, and H. Parvin, "Probabilistic planning of the active and reactive power sources constrained to securable-reliable operation in reconfigurable smart distribution networks," *Electr. Power Syst. Res.*, vol. 199, Oct. 2021, Art. no. 107457.

[16] F. H. Aghdam, S. Ghaemi, and N. T. Kalantari, "Evaluation of loss minimization on the energy management of multi-microgrid based smart distribution network in the presence of emission constraints and clean productions," *J. Cleaner Prod.*, vol. 196, pp. 185–201, Sep. 2018.

[17] M. Roustaee and A. Kazemi, "Multi-objective stochastic operation of multi-microgrids constrained to system reliability and clean energy based on energy management system," *Electr. Power Syst. Res.*, vol. 194, May 2021, Art. no. 106970.

[18] M. Roustaee and A. Kazemi, "Multi-objective energy management strategy of unbalanced multi-microgrids considering technical and economic situations," *Sustain. Energy Technol. Assessments*, vol. 47, Oct. 2021, Art. no. 101448.

[19] D. Wang, J. Qiu, L. Reedman, K. Meng, and L. L. Lai, "Two-stage energy management for networked microgrids with high renewable penetration," *Appl. Energy*, vol. 226, pp. 39–48, Sep. 2018.

[20] A. Azarhooshang, D. Sedighizadeh, and M. Sedighizadeh, "Two-stage stochastic operation considering day-ahead and real-time scheduling of microgrids with high renewable energy sources and electric vehicles based on multi-layer energy management system," *Electr. Power Syst. Res.*, vol. 201, Dec. 2021, Art. no. 107527.

[21] S. Pirouzi, J. Aghaei, T. Niknam, M. H. Khooban, T. Dragicevic, H. Farahmand, M. Korpas, and F. Blaabjerg, "Power conditioning of distribution networks via single-phase electric vehicles equipped," *IEEE Syst. J.*, vol. 13, no. 3, pp. 3433–3442, Sep. 2019.

[22] W. Jakob and C. Blume, "Pareto optimization or cascaded weighted sum: A comparison of concepts," *Algorithms*, vol. 7, no. 1, pp. 166–185, Mar. 2014.

[23] S. Pirouzi and J. Aghaei, "Mathematical modeling of electric vehicles contributions in voltage security of smart distribution networks," *Simulation*, vol. 95, no. 5, pp. 429–439, 2019.

[24] S. M. Mohseni-Bonab, A. Rabiee, and B. Mohammadi-Ivatloo, "Voltage stability constrained multi-objective optimal reactive power dispatch under load and wind power uncertainties: A stochastic approach," *Renew. Energy*, vol. 85, pp. 598–609, Jan. 2016.

[25] A. Shahbazi, J. Aghaei, S. Pirouzi, T. Niknam, M. Shafie-khah, and J. P. S. Catalão, "Effects of resilience-oriented design on distribution networks operation planning," *Electr. Power Syst. Res.*, vol. 191, Feb. 2021, Art. no. 106902.

[26] A. Shahbazi, J. Aghaei, S. Pirouzi, M. Shafie-khah, and J. P. S. Catalão, "Hybrid stochastic/robust optimization model for resilient architecture of distribution networks against extreme weather conditions," *Int. J. Electr. Power Energy Syst.*, vol. 126, Mar. 2021, Art. no. 106576.

[27] H. Hamidpour, J. Aghaei, S. Dehghan, S. Pirouzi, and T. Niknam, "Integrated resource expansion planning of wind integrated power systems considering demand response programmes," *IET Renew. Power Gener.*, vol. 13, no. 4, pp. 519–529, Mar. 2019.

[28] A. Rasouli, M. Bigdeli, and A. Samimi, "Robust PSO-based framework for concurrent active/reactive and reserve management in microgrids in the presence of energy storage systems," *Int. J. Energy Res.*, vol. 45, no. 13, pp. 19331–19350, Oct. 2021.

[29] A. Samimi and N. Rezaei, ''Robust optimal energy and reactive power management in smart distribution networks: An info-gap multi-objective approach,'' *Int. Trans. Electr. Energy Syst.*, vol. 29, no. 11, p. 12115, Nov. 2019.

[30] A. Samimi and H. Shateri, ''Network constrained optimal performance of DER and CHP based micro-grids within an integrated active-reactive and heat powers scheduling,'' *Ain Shams Eng. J.*, vol. 12, no. 4, pp. 3819–3834, Dec. 2021.

[31] A. Kavousi-Fard and T. Niknam, ''Optimal distribution feeder reconfiguration for reliability improvement considering uncertainty,'' *IEEE Trans. Power Del.*, vol. 29, no. 3, pp. 1344–1353, Jun. 2014.

[32] A. R. Malekpour, T. Niknam, A. Pahwa, and A. K. Fard, ''Multi-objective stochastic distribution feeder reconfiguration in systems with wind power generators and fuel cells using the point estimate method,'' *IEEE Trans. Power Syst.*, vol. 28, no. 2, pp. 1483–1492, May 2013.

[33] A. Kavousi-Fard and A. Khodaei, ''Efficient integration of plug-in electric vehicles via reconfigurable microgrids,'' *Energy*, vol. 111, pp. 653–663, Sep. 2016.

[34] P. R. Babu, C. P. Rakesh, M. N. Kumar, G. Srikanth, and D. P. Reddy, ''A novel approach for solving distribution networks,'' in *Proc. Annu. IEEE India Conf. (INDICON)*, Dec. 2009, pp. 1–5.

[35] S. Pirouzi, J. Aghaei, M. Shafie-khah, G. J. Osório, and J. P. S. Catalão, ''Evaluating the security of electrical energy distribution networks in the presence of electric vehicles,'' in *Proc. IEEE Manchester PowerTech*, Jun. 2017, pp. 1–6.

[36] S. Pirouzi, M. A. Latify, and G. R. Yousefi, ''Investigation on reactive power support capability of PEVs in distribution network operation,'' in *Proc. 23rd Iranian Conf. Electr. Eng.*, May 2015, pp. 1–6.

[37] *Generalized Algebraic Modeling Systems (GAMS)*. Accessed: Oct. 1, 2020. [Online]. Available: http://www.gams.com

[38] M. R. Ansari, S. Pirouzi, M. Kazemi, A. Naderipour, and M. Benbouzid, ''Renewable generation and transmission expansion planning coordination with energy storage system: A flexibility point of view,'' *Appl. Sci.*, vol. 11, no. 8, p. 3303, Apr. 2021.

[39] J. Aghaei, S. A. Bozorgavari, S. Pirouzi, H. Farahmand, and M. Korpås, ''Flexibility planning of distributed battery energy storage systems in smart distribution networks,'' *Iranian J. Sci. Technol., Trans. Electr. Eng.*, vol. 44, no. 3, pp. 1105–1121, Sep. 2020.

[40] M. Norouzi, J. Aghaei, S. Pirouzi, T. Niknam, and M. Lehtonen, ''Flexible operation of grid-connected microgrid using ES,'' *IET Gener., Transmiss. Distrib.*, vol. 14, no. 2, pp. 254–264, Jan. 2020.

FARID ADABI received the B.Sc. degree in electrical engineering from the K. N. Toosi University of Technology, Tehran, Iran, in 2007, the M.Sc. degree in electrical engineering from the Amirkabir University of Technology (Tehran Polytechnic), Tehran, in 2010, and the Ph.D. degree in electrical engineering from the Science and Research Branch of Islamic Azad University, Tehran, in 2016. He is currently an Assistant Professor with Islamic Azad University, Sanandaj Branch, Sanandaj, Iran. His main research interests include smart grid planning and operation, renewable energy systems, electric vehicles as well as electricity market structure and architecture.

ABDOLLAH KAVOUSI-FARD (Senior Member, IEEE) received the B.Sc. degree in electrical engineering from the Shiraz University of Technology, Shiraz, Iran, in 2009, the M.Sc. degree in electrical engineering from Shiraz University, Shiraz, in 2011, and the Ph.D. degree in electrical engineering from the Shiraz University of Technology, in 2016. He was a Researcher with the University of Denver, Denver, CO, USA, from 2015 to 2016, conducting research on microgrids. He was a Postdoctoral Research Assistant at the University of Michigan, Ann Arbor, MI, USA, from 2016 to 2018. He is currently an Assistant Professor at the Shiraz University of Technology. He has published more than 100 research papers in prestigious international journals and peer-reviewed conference proceedings. His current research interests include operation, management and cyber security analysis of smart grids, microgrid, smart city, electric vehicles as well as protection of power systems, reliability, artificial intelligence, and machine learning. He is an Associate Editor in Springer, *ISTE ISI Journal*, and the IEEE Transactions on Industrial Applications.

MEHDI VEISI received the M.Sc. degree in electrical engineering from the Science and Research Branch, Islamic Azad University, Tehran, Kurdistan, Iran. He has eight years of teaching experience, as a Visiting Lecturer with Islamic Azad University. His research interests include smart grid and microgrid, active distribution networks, bi-level optimization, power system operation, power system planning, electric vehicles energy management, renewable energy, and the Internet of Things.

MAZAHER KARIMI (Senior Member, IEEE) received the Ph.D. degree in electrical energy and power systems from the University of Malaya, Kuala Lumpur, Malaysia, in 2013.

He worked as a Research Associate with The University of Manchester, from 2016 to 2017. From 2017 to 2020, he was an Assistant Professor at Gonbad Kavous University, Iran. He is currently an Assistant Professor at the School of Technology and Innovations, University of Vaasa, Vaasa, Finland. His current research interests include smart grid applications, wide-area monitoring, protection, and control, distributed generation, power system stability, and frequency control.

● ● ●